

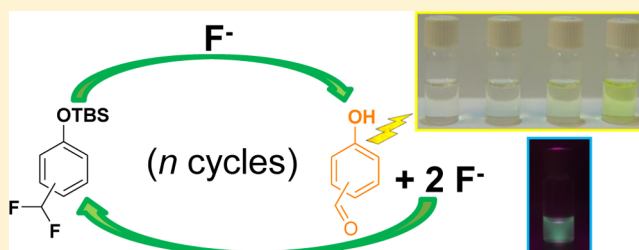
Minimal Self-Immolative Probe for Multimodal Fluoride Detection

Luca Gabrielli* and Fabrizio Mancin

Università di Padova, Dipartimento di Scienze Chimiche, via Marzolo 1, 35125 Padova, Italy

S Supporting Information

ABSTRACT: Two single-molecule, self-immolative fluoride probes, namely *tert*-butyldimethylsilyl-protected 2- and 4-difluoromethylphenol, are described. Compared to similar systems previously described, the probes are characterized by a simpler structure and straightforward, two-step preparation. Nevertheless, they allow the detection of fluoride ions at micromolar concentration by the naked eye, UV-vis absorption, and fluorescence. A detailed investigation of the self-immolative reaction reveals that the rate-limiting step is the release of the first fluoride ion from the difluoromethylphenolate intermediate. Moreover, the mutual position of the difluoromethyl- and *tert*-butyldimethylsilyl-protected residues has a relevant effect on the reactivity. Likely, a CF₂H–O hydrogen bond in the 2-isomer increases the reactivity of the silyl ether toward hydrolytic cleavage but also stabilizes the phenolate intermediate, slowing the release of fluoride ions.



INTRODUCTION

Signal amplification is a valuable strategy for the realization of effective chemosensors.¹ Indeed, it enables detection of very low analyte amounts by converting the recognition event into multiple signaling events. Several approaches have been explored, mainly involving catalysis and multivalency. Among them, molecular systems featuring autoinductive signal amplification^{2–9} represent a very promising strategy. Such probes feature a specific triggering group, which is selectively activated by the target analyte. This event starts a reaction where the activated probe decomposes, liberating both signal transduction molecules, which propagate the reaction by activating new trigger groups, and reporter molecules, which generate the readout signal.⁵ Such a cyclic reaction process results in signal amplification and consequent high sensitivity. Scientists call these probes “self-immolative”, since they structurally “sacrifice” themselves in order to perform their designated function.¹⁰ Several advantages are obtained with such systems: self-immolative probes grant high selectivity along with relatively low costs and high shelf stability. For this reason, they represent a valuable alternative to the most popular detection techniques, which rely on antibodies, enzymes, and other biomolecules.^{1a}

Among others, fluoride is a relevant target that can be detected with self-immolative probes with signal amplification. Fluoride content in drinking water should be below 4 ppm to avoid long-term exposure effects on teeth and bones. For this reason, several chemosensors and probes for fluoride have been reported over the years.¹¹ Among them, the number of self-immolative probes featuring signal amplification is quite limited. The first fluoride self-immolative probe was reported by Shabat in 2011^{12b} (Figure 1, a). The phenolate derivative formed by the fluoride-induced cleavage of the *tert*-butyldimethylsilyl (TBS) protecting group undergoes a series

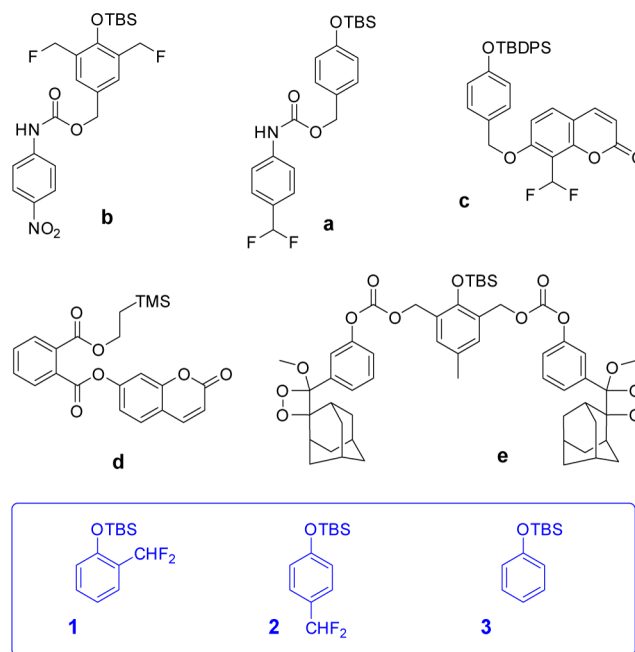


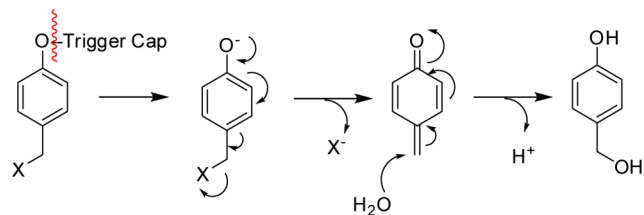
Figure 1. (Top) Self-immolative probes a–e for detection of fluorine reported in literature,^{2,12,13} self-immolative probes 1 and 2 presented in this work, and reference compound 3.

of quinone-methide rearrangement disassembling reactions (as in Scheme 1) that lead to the release of two fluoride anions and one 4-nitroaniline reporter, which absorbs light in the visible region (400 nm). The formation of two fluoride ions starts a

Received: July 26, 2016

Published: October 6, 2016

Scheme 1. Mechanism for the Self-Cleavage of 4-Methyl Halide Phenolate Derivatives (the 2-Substituted Derivatives Undergo a Similar Process)



cascade reaction that leads to the complete disassembly of the probe molecules present in the sample and the consequent signal amplification. Later on, Philips and co-worker described probe **b** (Figure 1) based on a similar sensing scheme.^{12b} In this case, cleavage of the TBS group initiates a disassembling reaction that generates 4-aminobenzaldehyde as a reporter group and two fluoride ions. In addition, probe **c**, recently reported by Huang and co-workers, uses the same working scheme.^{12a} In this case, beside the two fluoride ions, a coumarin molecule is formed. The use of fluorescence emission as a detection method led to a substantial improvement of the limit of detection with respect to the previous systems based on absorbance.

Probes **d** and **e** (Figure 1) detect fluoride by a self-immolative reaction using related working schemes. In the case of probe **d**, cleavage of the TMS group leads to the formation of coumarin phthalate monoester, which rapidly hydrolyzes to form coumarin. As in the previous case, the signal produced is an increase of the luminescence but no signal amplification is possible. In the case of probe **e**, the rearrangement reaction following the cleavage of the protecting group leads to the release of two adamantyl-3-hydroxyphenyl 1,2-diethoxyethane derivatives. These, in turn, decompose to form electronically excited 3-carboxymethyl phenolates that emit at 466 nm. In this way, chemiluminescence-based fluoride detection was possible, but signal amplification was limited to the generation of two reporter molecules per fluoride anion.

In general, the probes so far reported are quite complex, being in any case constituted by two components, namely a trigger and a signal generator,^{4,6} connected to form a single molecule.^{2,12} In this work, we designed, synthesized, and studied the new single-molecule self-immolative probes for fluoride anions **1** and **2** (Figure 1) based, respectively, on the 2- and 4-hydroxybenzaldehyde scaffolds. In contrast to previous examples, the detector and amplifier are not connected as subunits of a large molecule but are integrated in the same scaffold. This makes the synthesis of the probe easy and cost-effective. Moreover, different detection modes are enabled using the same probe, including naked eye, luminescence, and UV-vis spectroscopy.

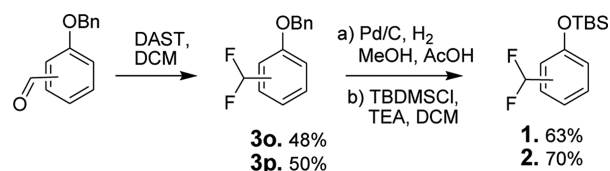
RESULTS AND DISCUSSION

Probes **1** and **2** are based, as in the example previously discussed, on the self-cleavage of 2- and 4-halomethyl phenolate derivatives (Figure 1). Following previous examples, we selected the *tert*-butyldimethylsilyl residue (TBS) as a trigger cap to protect the phenol moiety, which is known to be selectively cleaved by fluoride ion.⁴ The transducer unit is the difluoromethyl group in position 2 or 4. This ensures two advantages. First, two fluoride anions are released by each probe molecule in order to propagate and amplify the signal

transduction. Second, the species formed by the disassembling reaction are 2- or 4-hydroxybenzaldehyde that can be detected either by their absorbance in the UV-vis region or fluorescence emission.

We could develop a facile and straightforward two-step synthesis of the target compounds **1** and **2** (Scheme 2). The

Scheme 2. Synthesis of the Self-Immolative Chemosensors



conversion of a hydroxybenzaldehyde into a derivative featuring a difluoromethyl moiety and a silyl ether protected phenol group represents a nontrivial synthetic challenge. On one hand, the TBS ether is not stable under the conditions for carbonyl group fluorination. On the other hand, fluorination followed by silyl ether protection of the phenol group could be problematic due to the intrinsic instability of the intermediate. Hence, we decided to use a temporary protecting group for the phenol moiety. Commercially available 2- and 4-(benzyloxy)benzaldehydes were converted into difluoromethyl derivatives with diethylaminosulfur trifluoride (DAST) in dichloromethane (DCM). The obtained fluorinated compounds (**3o** and **3p**, Scheme 2) were debenzylated by hydrogenolysis under acidic conditions in order to minimize the disassembly of the unstable phenolate and then reacted with the *tert*-butyldimethylsilyl chloride (TBSCl) obtaining the desired compounds **1** and **2**. Compound **3** (Figure 1) was also prepared, as a control molecule, by reacting phenol with TBSCl in DCM (see the SI for details). Derivatives **1** and **2** are stable at room temperature, and when stored at 4 °C, they did not show any hydrolysis for at least one year.

In a series of experiments aimed at testing their capability to detect fluoride, using tetrabutylammonium fluoride (TBAF) as a F⁻ source, we found that the best solvent for the self-amplified reaction is a mixture of organic polar solvents, water, and trimethylamine as a base (DMSO/ACN/H₂O/triethylamine 47:47:5:0.5). Consequently, we investigated the fluoride-dependent signal generation by incubating probe **1** (500 μM) with different concentrations of fluoride and monitoring the increase of absorbance at 400 nm (Figure 2A), which corresponds to the absorption maximum of 2-hydroxyaldehyde

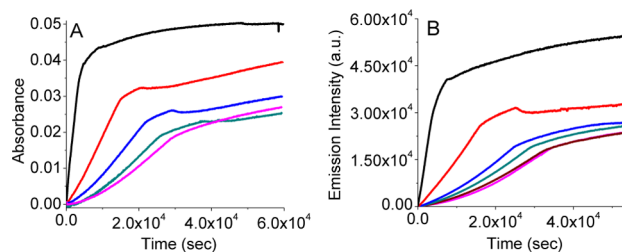


Figure 2. UV-vis absorbance (A, 400 nm) and fluorescence emission (B, $\lambda_{\text{exc}} = 400 \text{ nm}$, $\lambda_{\text{em}} = 483 \text{ nm}$) traces at 400 nm for the reaction of probe **1** (500 μM) with different amounts of tetrabutylammonium fluoride (black, 250 μM; red, 100 μM; blue, 50 μM; green, 25 μM; dark red, 10 μM; magenta, background). Conditions: DMSO/ACN/H₂O/triethylamine 47:47:5:0.5, 25 °C.

at the highest wavelength. Kinetic profiles recorded follow different trends. At high fluoride concentration (250 μM), the absorbance rapidly increases to level off at a plateau value after about 100 min. At lower concentrations, the absorbance increase follows initially an exponential profile to level off later. As will be discussed in detail later, such behavior is due to the presence of different species absorbing at this wavelength. The exponential absorbance increase, observed in the first phase of the experiments at low fluoride concentration, is coherent with the amplification process. When the kinetic profiles are compared with the background degradation of **1** under the same conditions (Figure 2A), a detection limit of 25 μM can be established that compares well with those obtained by similar systems.^{2,12,13} Interestingly, we found that the signal produced, i.e., the absorbance of the solution after the degradation of **1**, can be increased by adding Cs_2CO_3 to the mixture. Figure 3

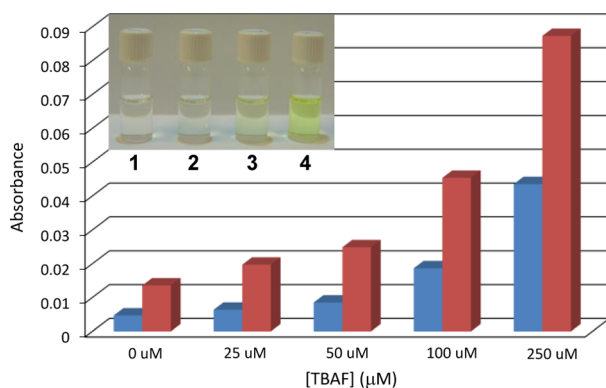


Figure 3. Absorbance improvement at 400 nm due to addition of Cs_2CO_3 (500 μM) to probe **1** (500 μM) at different F^- concentrations. Inset: picture of the samples after Cs_2CO_3 addition; 1, control; 2, 50 μM F^- ; 3, 100 μM F^- ; 4, 250 μM F^- . Conditions: DMSO/ACN/ H_2O /triethylamine 47:47:5:0.5, 180 min, 25 $^\circ\text{C}$.

reports the values of the absorbance at 400 nm recorded for 500 μM solutions of **1** incubated for 180 min with different amounts of fluoride, before and after the addition of the cesium salt. In each case, the absorbance is 2-fold increased, and fluoride can be detected by the naked eye at 100 μM concentration. Fluoride detection was also investigated by monitoring fluorescence emission of 2-hydroxyaldehyde at 483 nm. (Figure 2B). Profiles observed are similar to the one recorded by UV-vis spectroscopy, and the detection limit remains 25 μM . Under these conditions, probe sensitivity appears to be mainly controlled by the background degradation rate and not by the detection technique used.¹⁴

The behavior of probe **2** is similar with a few remarkable differences. Figure 4A reports the absorbance profiles obtained by incubation of **2** with different amounts of fluoride under the same conditions used for **1**. Here, the highest absorption maximum of the degradation products (mainly 4-hydroxybenzaldehyde) is at 345 nm. The kinetic profiles are similar to those observed for probe **1**, with the only difference being that the initial absorbance increase appears to be faster. In this case, the minimal detectable fluoride concentration is 25 μM .

The probes selectivity was investigated by probe **1** with different anions each at 100 μM concentration (Figure 5).¹⁵ In any case, signal produced by all ions but fluoride was superimposable with the background signal.^{4,16,17} On the

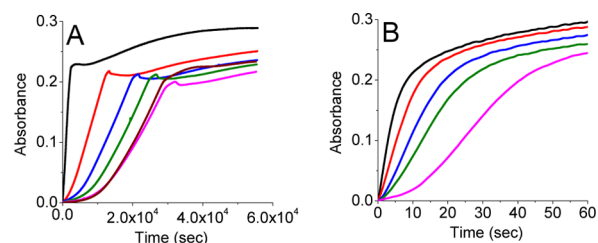


Figure 4. UV-vis absorbance traces at 345 nm for the reaction of probe **2** (500 μM) with different amounts of tetrabutylammonium fluoride (black, 250 μM ; red, 100 μM ; blue, 50 μM ; green, 25 μM ; dark red, 10 μM ; magenta, background). Conditions: (A) DMSO/ACN/ H_2O /triethylamine 47:47:5:0.5, 25 $^\circ\text{C}$; (B) DMSO/ACN/ H_2O 37:37:25, 50 $^\circ\text{C}$.

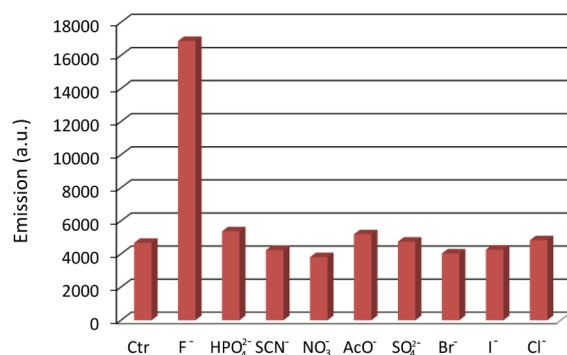


Figure 5. Fluorescence emission intensity ($\lambda_{\text{exc}} = 400$ nm, $\lambda_{\text{em}} = 483$ nm) upon incubation of probe **1** (500 μM) with different anions. Conditions: DMSO/ACN/ H_2O /triethylamine 47:47:5:0.5, 25 $^\circ\text{C}$.

other hand, in the presence of fluoride, the signal measured is 4-fold more intense.

A deeper understanding of the process was obtained by investigating the probe degradation process by NMR spectroscopy under the same conditions as the UV-vis and fluorescence experiments (Figure 5). According to the commonly accepted mechanisms for the self-immolative reaction, several species were detected in ^1H NMR and ^{19}F NMR experiments (see the SI, section 3). Figure 5 reports the time-dependent concentration changes of the most relevant species detected in the case of probes **1** and **2** incubated at 500 μM concentration with 25 μM fluoride. The profiles could be fitted according to the mechanism reported in Figure 6. The first step of the reaction is the cleavage of the silyl ether, which is completed within 10 h in the case of **1** and within 7 h in the case of **2**. As a result of this reaction, three products are formed: (a) 2- or 4-(difluoromethyl)phenolate (**II**), (b) *tert*-butyldimethylsilyl fluoride (TBSF), and (c) *tert*-butyldimethylsilanol (TBSOH). The latter two products are detected in the spectral region between -0.1 and $+0.3$ ppm, as expected for alkylsilane derivatives. The amount of TBSF formed at the end of the reaction (about 250–400 μM) is much greater than the amount of fluoride initially present. This confirms the occurrence of the self-immolative reaction with the additional fluoride yielded by the decomposition of the phenolate **II**. Moreover, the concentrations of TBSF and TBSOH remain almost constant for at least 10 h after the complete deprotection of **1** and **2**. TBSOH is hence a relatively stable species in the reaction conditions and is formed only marginally by hydrolysis of TBSF in the time span of the experiments. The pseudo-first-order rate constant for the hydrolysis of TBSF obtained by the

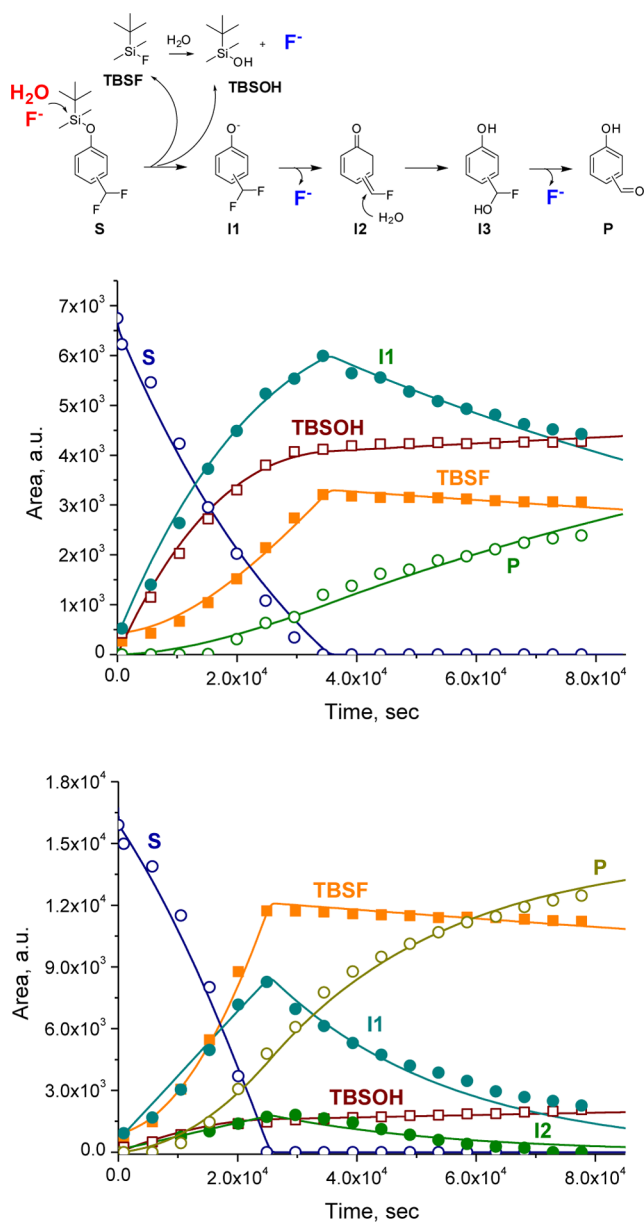


Figure 6. ^1H NMR kinetic study of $500\ \mu\text{M}$ probes **1** (upper) and **2** (lower) reaction with TBAF ($25\ \mu\text{M}$). The normalized area of characteristic compound peaks is plotted vs reaction time. Conditions: $\text{DMSO-}d_6$: $\text{CD}_3\text{CN}/\text{D}_2\text{O}/\text{triethylamine}$ 47:47:5:0.5, $28\ ^\circ\text{C}$.

interpolation of the kinetic profiles is about $2.2 \times 10^{-6}\ \text{s}^{-1}$. TBSF and TBSOH are consequently the products of two concurrent deprotection reactions. In the first one, the TBS group is cleaved as planned by fluoride. This reaction is very fast (diffusion controlled according to the fittings) but is limited by the availability of fluoride in the samples. In the second reaction, the TBS groups is cleaved by hydroxide anions or water molecules present in the reaction mixture. Interestingly, the formation of TBSOH is more relevant in the case of **1**. Indeed, the rates for the hydrolysis of the protecting group are, respectively, $4.2 \times 10^{-5}\ \text{s}^{-1}$ and $2.4 \times 10^{-5}\ \text{s}^{-1}$ for **1** and **2**.

The concentration of **I1** increases as the result of the TBS deprotection, reaching a maximum after 7–10 h. The following decrease is due to the self-cleavage of the C–F bonds to form the final salicylates. Notably, neither of the subsequent intermediates (hydroquinone **I2** and the α -hydroxyfluoro

intermediate **I3**, Figure 5) was detected in the self-cleavage of **1**, suggesting that these species are quite reactive and the rate-limiting step is the first C–F cleavage. On the other hand, decomposition of **I1** is much faster for **2** ($3.3 \times 10^{-5}\ \text{s}^{-1}$) than for **1** ($8.8 \times 10^{-6}\ \text{s}^{-1}$), and this allows, in the case of **2**, the accumulation of the hydroquinone intermediate **I2**, whose decomposition is still very fast ($5 \times 10^{-3}\ \text{s}^{-1}$), as expected. Nicely enough, the reaction rates obtained by the fit of the NMR experiments allowed us to interpolate the UV–vis kinetic experiments, with both **I1** and the final hydroxyaldehydes contributing to the absorption increase.

In order to further investigate the deprotection process, we also performed ^1H NMR kinetic experiments with reference compound **3** (Figure 1), which is devoid of the difluoromethyl group. In the presence of F^- ($25\ \mu\text{M}$) (Figures S7 and S8), as expected, we did not observe any amplification, and only the 5% of **3** reacted to give phenol since no more fluoride was available to propagate the reaction. Hence, signal amplification allowed by probes **1** and **2** with respect to **3** under this conditions is 20-fold.¹⁸

Relevant information is provided by the above experiments: (1) the background reaction that determines the detection limit of the probes is the hydrolysis of the TBS group; (2) the presence of the difluoromethyl group increases the lability of the TBS-protected phenol; this is likely due to the electron-withdrawing ability of the substituent that decreases the basicity of the resulting phenolate; (3) the effect is stronger when the difluoromethyl group is in the ortho position, and the decomposition of the resulting **I1** intermediate is slower. This behavior suggests an additional phenolate stabilization that can likely arise by an intramolecular $\text{CF}_2\text{H}-\text{O}^-$ hydrogen bond.

One of the main limitations of self-immolative probes is the long time required for the analysis, which is generally in the range of hours. Our results demonstrate that the rate limiting step is the first quinone-methide rearrangement. For this reason, phenolate intermediates accumulate in the early part of the reaction and both signal-producing species and signal-amplifying fluoride are produced in small amounts. The stabilization of the phenolate oxygen may further decrease the reaction rate. However, we found that reaction times can be sensibly decreased by increasing the temperature. At $50\ ^\circ\text{C}$, maximum absorbance is reached within 30 min with both probes. Nicely enough, in the case of probe **2**, the background reaction is much less sensitive to the temperature increase than the fluoride-initiated reaction. This allowed a decrease of the detection limit to $5\ \mu\text{M}$.

Another relevant drawback is the requirement of a highly organic solvent system for the self-immolative reactions. Such a problem can be addressed easily when the reaction is performed at higher temperature. Indeed, working at $50\ ^\circ\text{C}$, we could simplify the solvent system to $\text{ACN}/\text{DMSO}/\text{H}_2\text{O}$ 37:37:25, simultaneously increasing the amount of water present in the reaction mixture. The detection limit in these operating conditions is $25\ \mu\text{M}$ for both probes, while the F^- detection time is reduced to about 10 min (Figure 4B and SI). It is worth mentioning that, since the water content reaches the 25%, the detection limit in the analyzed water sample reaches 1.9 ppm ($100\ \mu\text{M}$), which is below the US Environmental Protection Agency's (EPA) recommended fluoride concentration in water (2 ppm) as well as the EPA's mandatory upper limit (4 ppm).¹⁹

CONCLUSION

In conclusion, we have shown that salicylaldehyde and its para isomer can be successfully used as scaffolds and reporters for building up new self-immolative constructs through a facile and straightforward two-step synthesis, starting from cheap compounds. Indeed, **1** and **2** are, to the best of our knowledge, the simplest single-molecule fluoride chemosensors so far reported. The sensing system is able to detect fluoride anions down to 25 μM , both by UV-vis absorption and fluorescence, through an autoinductive signal amplification reaction. Naked eye detection is also possible with a threshold value of 100 μM . For the first time, the self-immolative mechanism was proven and extensively studied by NMR kinetic experiments. Experiments confirmed the amplification mechanism and revealed that the rate-determining step of the reaction is the decomposition of the phenolate intermediate with concurrent release of one fluoride ion. On the other hand, the limit of the detection is controlled by the hydrolytic resistance of the triggering cup. In further evolutions, the probe sensitivity could be improved by increasing the stability of the cap. Moreover, these chemosensors could work as amplifiers in a two-component analyte detector system as the simple synthetic strategy setup opens a wide range of possibilities. By modifying only the last synthetic step and protecting the hydroxyl moiety with an appropriate group, it could be, in principle, possible to prepare a probe for almost any desired analyte.

EXPERIMENTAL SECTION

General Methods. Solvents were purified by standard methods. All commercially available reagents and substrates were used as received. TLC analyses were performed using F₂₅₄ precoated silica gel glass plates. Column chromatography was carried out on silica gel 60 (70–230 mesh). Pt/C was filtered by 25 mm syringe filter with a 0.45 μm nylon membrane. NMR spectra were recorded using a spectrometer operating at 500 MHz for ¹H and 125.8 MHz for ¹³C. Chemical shifts are reported relative to internal Me₄Si. ¹⁹F NMR spectra were acquired using a spectrometer operating at 400 MHz for ¹H and 376 MHz for ¹⁹F, equipped with a probe QNP 5 mm. Multiplicity is given as follows: s = singlet, d = doublet, t = triplet, q = quartet, qn = quintet, m = multiplet, br = broad peak. GC-MS mass spectra were obtained using a (5% phenyl)methylpolysiloxane capillary column 30 cm long, I.D. 0.25, film 0.25 μm , He as the carrier gas, and the following settings: inlet 250 °C, oven ramp 3 min, 50 °C, 15 °C/min, 10 min 250 °C. UV-vis spectra were recorded with a double-beam spectrophotometer using an average time of 0.0125s, data interval 5 nm, scan rate 24000 nm/min. Fluorescence spectra were recorded using a plate reader; excitation 400 nm, emission 483 nm, excitation bandwidth 10 nm, emission bandwidth 5 nm, gain 93, no. of flashes 50, flash frequency 400 Hz, integration time 20 μs , lag time 0 μs , settle time 100 ms.

General Procedure for Sensing Experiments. The reported disassembly reactions were performed as follows: 5 μL of a 50 mM DMSO stock solution of the desired probe was diluted with 229 μL of DMSO and 234 μL of acetonitrile (ACN), and then water (25 μL) and triethylamine (2.5 μL) were added. Finally, to this solution we added 5 μL of a freshly prepared TBAF solution in THF. The mixture was vigorously shaken for few seconds and then incubated at room temperature. For NMR experiments, deuterated DMSO, D₂O, and ACN were used. Fresh TBAF solutions were prepared by dissolving the required amount of TBAF \times 3H₂O in dry THF. The DMSO probe's stock solution was stored at -18 °C. We performed the disassembly reactions in 1.5 mL Eppendorf plastic vials in order to avoid glass interference in the catalytic amount of fluoride. For the NMR studies, the mixture was further transferred into a well-sealed NMR tube.

General Procedure for Intermediates **3o and **3p**.** Benzyloxibenzaldehyde (430 mg, 2.026 mmol, 1 equiv) was dissolved in dry DCM (1 mL), and then catalytic MeOH (1.5 μL) and DAST (495 μL , 5.065 mmol, 2.5 equiv) were added. The reaction was stirred at room temperature under N₂ atmosphere for 3 days. The reaction was quenched by adding a Na₂CO₃-saturated solution, until neutralization, the product was extracted in DCM, and the organic layers were collected, dried over MgSO₄, and finally purified by flash column chromatography (from 9.5:0.5 to 8:2 hexane/EtOAc) to afford the fluorinated product (as a colorless oil) and the unreacted aldehyde. Although the reaction time is prolonged, the reaction is clean since the desired fluorinated product is the only product formed and the unreacted starting compound can be easily recovered.

1-(Benzyloxy)-2-(difluoromethyl)benzene (3o**):** 228 mg, yield 48%; ¹H NMR (200 MHz, CDCl₃) δ 7.68 (d, *J* = 7.6 Hz, 1H), 7.56–7.37 (m, 6H), 7.18–7.02 (m, 2H), 7.12 (t, *J*_{HF} = 55.7 Hz, 1H), 5.20 (s, 2H); ¹³C NMR (50 MHz, MeOD) δ 156.9, 136.8, 132.2, 128.9, 128.4, 127.5, 126.6 (t, ²*J*_{CF} = 5.8 Hz), 121.2, 112.6, 111.9 (t, *J*_{CF} = 235.7 Hz), 70.6; ¹⁹F NMR (376 MHz, CDCl₃) δ -115.68 (d, *J* = 55.7 Hz); GC-MS (EI) *m/z* 234 (M⁺), 91 (PhCH₂⁺), 51 (CHF₂⁺).²⁰

1-(Benzyloxy)-4-(difluoromethyl)benzene (3p**):** 237 mg, yield 50%; ¹H NMR (300 MHz, CDCl₃) δ 7.58–7.32 (m, 7H), 7.07 (d, *J* = 8.5 Hz, 2H), 6.63 (t, *J*_{HF} = 56.7 Hz, 1H), 5.13 (s, 2H); ¹³C NMR (75 MHz, CDCl₃) δ 160.6, 136.5, 128.7, 128.2, 127.5, 127.2 (t, ²*J*_{CF} = 5.7 Hz), 115.0 (2C), 114.9 (t, *J*_{CF} = 237.0 Hz), 70.1; ¹⁹F NMR (376 MHz, CDCl₃) δ -108.72 (d, *J* = 56.7 Hz); GC-MS (EI) *m/z* 234 (M⁺), 91 (PhCH₂⁺), 51 (CHF₂⁺).²⁰

General Procedure for Compounds **1 and **2**.** Compound **3o/3p** (197 mg, 0.841 mmol, 1 equiv) was dissolved in MeOH (2 mL), AcOH (100 μL) and Pd/C (180 mg) were added, and then the solution was degassed in vacuum under stirring. Finally, H₂ was added, and the mixture was vigorously stirred for 1.5 h. After the reaction was complete, Pd was filtered off with a syringe filter, the solvent was evaporated under reduced pressure, and the product was dissolved in dry DCM (2 mL). TEA (470 μL , 3.364 mmol, 4 equiv) and TBDMSCl (253 mg, 1.682 mmol, 2 equiv) were quickly added, and the mixture was reacted under N₂. After 2 h, silica was added, the solvent was evaporated, and the product was finally purified by flash column chromatography (9.5:0.5 EP/EtOAc) to afford the final compound as a colorless oil.

tert-Butyl(2-(difluoromethyl)phenoxy)dimethylsilane (1**):** 137 mg, yield 63%; ¹H NMR (200 MHz, CDCl₃) δ 7.61 (d, *J* = 7.5 Hz, 1H), 7.37 (d, *J* = 7.4 Hz, 1H), 7.08 (t, *J* = 7.4 Hz, 1H), 6.98 (t, *J*_{HF} = 55.8 Hz, 1H), 6.91 (d, *J* = 8.2 Hz, 1H), 1.08 (s, 9H), 0.32 (s, 6H); ¹³C NMR (50 MHz, MeOD) δ 154.0, 131.9 (2C), 126.7 (t, ²*J*_{CF} = 5.6 Hz), 121.4, 119.1, 112.1 (t, *J*_{CF} = 236.0 Hz), 25.8, 18.4 (3C), -4.1 (2C); ¹⁹F NMR (376 MHz, DMSO/ACN 1:1, D₂O 5%, TEA 0.5%) δ -118.89 (d, *J*_{FH} = 55.8 Hz); ²⁹Si NMR (99 MHz, CDCl₃) δ 22.68; GC-MS (EI) *m/z* 258 (M⁺), 201 ([M - tBu]⁺), 57 (tBu⁺).²⁰

tert-Butyl(4-(difluoromethyl)phenoxy)dimethylsilane (2**):** 152 mg, yield 70%; ¹H NMR (300 MHz, CDCl₃) δ 7.40 (d, *J* = 8.3 Hz, 2H), 6.91 (d, *J* = 8.4 Hz, 2H), 6.60 (t, *J*_{HF} = 56.8 Hz, 1H), 1.01 (s, 9H), 0.23 (s, 6H); ¹³C NMR (75 MHz, CDCl₃) δ 157.8, 127.1 (2C), 120.2 (2C), 114.9 (t, *J*_{CF} = 237.5 Hz), 25.6, 18.2, -4.4; ¹⁹F NMR (377 MHz, DMSO/ACN 1:1, D₂O 5%, TEA 0.5%) δ -112.08 (d, *J*_{FH} = 56.8 Hz); ²⁹Si NMR (99 MHz, CDCl₃) δ 21.84; GC-MS (EI) *m/z*: 201 ([M - tBu]⁺), 77 (Ph⁺), 57 (tBu⁺).²⁰

[(1,1-Dimethylethyl)dimethylsilyloxy]benzene (3**):** Phenol (200 mg, 2.125 mmol, 1 equiv) was dissolved in dry DCM (10 mL); TEA (323 μL , 3.190 mmol, 1.5 equiv) and TBDMSCl (481 mg, 3.190 mmol, 1.5 equiv) were added with stirring, and the mixture was reacted under N₂ for 6 h. Silica was added, the solvent was evaporated, and the product was finally purified by flash column chromatography (100% EP) to afford the protected phenol **3** as a clear oil (376 mg, 85% yield): ¹H NMR (200 MHz, CDCl₃) δ 7.24 (t, *J* = 7.8 Hz, 2H), 6.96 (t, *J* = 7.4 Hz, 1H), 6.86 (d, *J* = 7.5 Hz, 2H), 1.01 (s, 9H), 0.22 (s, 6H); ¹³C NMR (50 MHz, CDCl₃) δ 155.8, 129.6 (2C), 121.5, 120.4 (2C), 25.9 (3C), 18.3, -4.19 (2C). (Data in agreement with those reported in literature.)²¹

■ ASSOCIATED CONTENT

■ Supporting Information

The Supporting Information is available free of charge on the ACS Publications website at DOI: 10.1021/acs.joc.6b01787.

Additional ^1H , ^{19}F NMR and UV experiments (PDF)

■ AUTHOR INFORMATION

Corresponding Author

*E-mail: luca.gabrielli@unipd.it.

Notes

The authors declare no competing financial interest.

■ ACKNOWLEDGMENTS

This work was supported by the ERC Starting Grants Project MOSAIC (259014) and by Università di Padova (Progetto Strategico di Ateneo NAMECA).

■ REFERENCES

- (1) (a) Scrimin, P.; Prins, L. *J. Chem. Soc. Rev.* **2011**, *40*, 4488. (b) Lei, J.; Ju, H. *Chem. Soc. Rev.* **2012**, *41*, 2122. (c) Makhlynets, O. V.; Korendovych, I. V. *Biomolecules* **2014**, *4*, 402.
- (2) Turan, I. S.; Akkaya, E. U. *Org. Lett.* **2014**, *16*, 1680.
- (3) Karton-Lifshin, N.; Shabat, D. *New J. Chem.* **2012**, *36*, 386.
- (4) Baker, M. S.; Phillips, S. T. *J. Am. Chem. Soc.* **2011**, *133*, 5170.
- (5) Sella, E.; Lubelski, A.; Klafter, J.; Shabat, D. *J. Am. Chem. Soc.* **2010**, *132*, 3945.
- (6) Sella, E.; Weinstain, R.; Erez, R.; Burns, N. Z.; Baran, P. S.; Shabat, D. *Chem. Commun.* **2010**, *46*, 6575.
- (7) Avital-Shmilovici, M.; Shabat, D. *Bioorg. Med. Chem.* **2010**, *18*, 3643.
- (8) Sella, E.; Shabat, D. *J. Am. Chem. Soc.* **2009**, *131*, 9934.
- (9) Zhu, L.; Anslyn, E. V. *Angew. Chem., Int. Ed.* **2006**, *45*, 1190.
- (10) Gnaim, S.; Shabat, D. *Acc. Chem. Res.* **2014**, *47*, 2970.
- (11) (a) Zhou, Y.; Zhang, J. F.; Yoon, Y. *Chem. Rev.* **2014**, *114*, 5511 and references cited therein. (b) Xiong, Y.; Wang, C.; Tao, T.; Duan, M.; Tan, J.; Wu, J.; Wang, D. *Analyst* **2016**, *141*, 3041. (c) Basu, A.; Suryawanshi, A.; Kumawat, B.; Dandia, A.; Guin, D.; Ogale, S. B. *Analyst* **2015**, *140*, 1837.
- (12) (a) Gu, J. A.; Mani, V.; Huang, S. T. *Analyst* **2015**, *140*, 346. (b) Perry-Feigenbaum, R.; Sella, E.; Shabat, D. *Chem. - Eur. J.* **2011**, *17*, 12123. (c) Baker, M. S.; Phillips, S. T. *Org. Biomol. Chem.* **2012**, *10*, 3595.
- (13) Mahoney, K. M.; Goswami, P. P.; Winter, A. H. *J. Org. Chem.* **2013**, *78*, 702.
- (14) Avital-Shmilovici, M.; Shabat, D. *Soft Matter* **2010**, *6*, 1073.
- (15) Similar results were obtained with probe 2; see the [Supporting Information](#).
- (16) Kim, S. Y.; Hong, J.-I. *Org. Lett.* **2007**, *9*, 3109.
- (17) Zhu, C.-Q.; Chen, J.-L.; Zheng, H.; Wu, Y.-Q.; Xu, J.-G. *Anal. Chim. Acta* **2005**, *539*, 311.
- (18) The extent of amplification depends both on the analyte and probe concentrations. In general, the signal produced by a non-immolative system is proportional to the analyte concentration, while the signal produced by a self-immolative system is proportional to the probe concentration. Signal amplification is consequently the ratio of the two values.
- (19) EPA National Primary Drinking Water Standards. See <https://www.epa.gov/dwstandardsregulations> for more information, accessed July 2016.
- (20) High-resolution mass spectra (HR-MS) were recorded on both an API-TOF mass spectrometer and on a Q-TOF (MeOH, 0.5% formic acid). However, we could not detect the molecular ion because the analytes were not ionizable under these analytical conditions. On the other hand, the volatility and oily nature of the reported molecules, together with the presence of F, Si, and O atoms, did not allow for meaningful elemental analysis (CHN microanalyzer). Ionization and

consequent detection of the compounds was possible only with a GC-MS (EI) spectrometer. In particular, the molecular ion and significant fragments (i.e., $[\text{M} - \text{tBu}]^+$) were detectable. Considering the simple nature of the compound and the fact that we have obtained the ^1H , ^{13}C , ^{19}F , and ^{29}Si NMR spectra as well as the GC-MS traces, we are confident of both the purity and identity of the compounds reported.

(21) Baker, M. S.; Phillips, S. P. *J. Am. Chem. Soc.* **2011**, *133*, 5170.